Clin Physiol Funct Imaging (2018) **38**, pp87–92 doi: 10.1111/cpf.12387

Impact of abnormal cerebrovascular reactivity on BOLD fMRI: a preliminary investigation of moyamoya disease

Erin L. Mazerolle[1], Yuhan Ma[2], David Sinclair[3] and G. Bruce Pike[1,2,3]

[1]*Department of Radiology, Hotchkiss Brain Institute, University of Calgary, Calgary, AB,* [2]*Department of Biomedical Engineering, McGill University, and* [3]*Department of Neurology and Neurosurgery, McGill University, Montreal, QC, Canada*

Correspondence
Erin L. Mazerolle, Department of Radiology, Hotchkiss Brain Institute, University of Calgary, Room 2905, Health Sciences Centre, 3330 Hospital Drive NW, Calgary, AB T2N 4N1, Canada
E-mail: erin.mazerolle@ucalgary.ca

Accepted for publication
Received 5 May 2016;
accepted 26 July 2016

Key words
cerebrovascular disease; functional brain mapping; hypercapnia; neurovascular coupling; stenosis

Summary

Blood oxygen level-dependent (BOLD) functional magnetic resonance imaging (fMRI) studies of patients with cerebrovascular disease have largely ignored the confounds associated with abnormal cerebral blood flow, vascular reactivity and neurovascular coupling. We studied BOLD fMRI activation and cerebrovascular reactivity in moyamoya disease. To characterize the impact of remote vascular demands on BOLD fMRI measurements, we varied the vascular territories engaged by manipulating the experimental task performed by the participants. Vascular territories affected by disease were identified using BOLD cerebrovascular reactivity. Preliminary evidence from two patients pre- and postrevascularization surgery and four controls indicates that neurovascular coupling in affected brain regions can be modulated by the task-related vascular demands in unaffected regions. In one patient studied, we observed that brain regions with improved cerebrovascular reactivity after surgery demonstrated normalized neurovascular coupling, that is the degree to which neurovascular coupling was modulated by task-related vascular demands was decreased. We propose that variations in task-dependent neurovascular coupling in patients with moyamoya disease are likely related to vascular steal. While preliminary, our findings are a proof of concept of the limitations of BOLD fMRI in cerebrovascular disease and suggest a role for assessment of cerebrovascular reactivity to improve interpretation of task-related BOLD fMRI activation.

Introduction

Blood oxygen level-dependent (BOLD) fMRI has become the leading tool to map human brain functions because it is a safe and sensitive technique for detecting brain activation. However, because the BOLD signal reflects the balance between hemodynamic and metabolic changes that accompany brain activation, rather than the neural activity itself, interpretation of BOLD signals is not always straightforward. This is particularly true for diseases in which cerebral hemodynamics are compromised (Pike, 2012). Nonetheless, patients with cerebrovascular diseases have been widely studied with BOLD fMRI, for example to track reorganization and recovery of brain function following an ischaemic event (reviewed previously, e.g. Calautti & Baron, 2003; Hodics *et al.*, 2006; Stinear, 2010; Richards *et al.*, 2008). While these studies often demonstrate differences between patients and controls, and may be pragmatically useful, the origin of BOLD differences (i.e. neural or vascular) cannot be definitively inferred (Veldsman *et al.*, 2015). This limits potential applications of BOLD for understanding neural plasticity associated with disease, treatment and recovery.

BOLD measurement of cerebrovascular reactivity (CVR) is emerging as a potential tool for characterizing pathology in cerebrovascular disease (e.g. Sam *et al.*, 2014; Geranmayeh *et al.*, 2015; Blair *et al.*, 2016). CVR is probed by administering a vasodilatory stimulus (e.g. inhaled CO_2) while BOLD images are collected (Spano *et al.*, 2013). The BOLD signal increase primarily reflects the vasculature's capacity to respond to increased demands, because at CO_2 levels typically applied in human MRI studies, oxygen metabolism changes are not significant (Chen & Pike, 2010), although changes in neural activity associated with CO_2 challenges have been observed in animals (e.g. Zappe *et al.*, 2008). Negative CVR is a sensitive marker of cerebrovascular dysfunction, suggesting vascular steal (Poublanc *et al.*, 2013). It has been proposed that vascular steal arises in areas of hypoperfusion in which the vessels are chronically dilated. This chronic dilation is thought to serve as a compensatory mechanism secondary to the hypoperfusion, but leaves the affected regions unable to respond to

further increased perfusion demands (Scott & Smith, 2009; Mikulis, 2013; Sobczyk *et al.*, 2014). Thus, when vessels in other regions dilate, blood flow is effectively stolen from regions in which vessels cannot further dilate (but see Arteaga *et al.*, 2014), leading to a negative BOLD response.

In this study, we extended the concept of pathological vascular steal to task-based fMRI. We evaluated whether task-related hemodynamic responses in regions with impaired CVR can be affected by the vascular demands in other brain regions. Analogously to how global vasodilators result in a redistribution of blood flow favouring unaffected regions, blood flow redistribution associated with brain activity in unaffected regions may have an impact on the hemodynamic response to brain activity in affected regions. In the context of the task-based fMRI with relatively modest vascular demands, such phenomena could have important implications for designing and interpreting fMRI studies in patients with cerebrovascular disease.

While moyamoya disease (MMD) is rare in North America (Uchino *et al.*, 2005), it provides an opportunity to consider the impact of remote vascular demands on brain regions with impaired CVR due to the spatial distribution of MMD pathology. MMD is associated with stenosis of the internal carotid, middle cerebral and/or anterior cerebral arteries. As a result, CVR in anterior brain regions tends to be abnormal, whereas CVR in posterior regions tends to be relatively spared (Burke *et al.*, 2009; but see Miki *et al.*, 2000 for a case study of an MMD patient with abnormal BOLD fMRI activation in posterior regions). In cases with this distribution of pathology, it is possible to probe normal (e.g. primary visual cortex) and abnormal (e.g. primary sensorimotor cortex) hemodynamic responses within individual patients with MMD using simple, robust fMRI tasks such as viewing flashing checkerboards and finger tapping.

We present preliminary evidence from two patients with MMD, pre- and postrevascularization surgery, and four controls demonstrating that in affected anterior regions, neurovascular uncoupling can arise from increased task-related vascular demands in unaffected posterior brain regions. Participants performed a separate motor task targeting affected anterior regions, and a combined visual–motor task. The combined task was designed to elicit the same neural activity in the primary sensorimotor cortex as the motor task, but with increased vascular demands in unaffected posterior brain regions. This experimental design allowed us to attribute BOLD response differences between the separate and combined tasks in the sensorimotor cortex to neurovascular coupling differences, rather than differences in underlying neural activity.

Methods

Participants

Two adult MMD patients with stenosis primarily affecting the right hemisphere were studied. Patient 1, a 48-year-old woman, participated preoperatively (extracranial-intracranial bypass) and 6 months postoperatively. Preoperatively, the patient experienced repeat episodes of left hemiparesis and cold sensation. Preoperative CT angiography/perfusion showed narrowed bilateral internal carotid and middle cerebral arteries and delayed time-to-peak of the right anterior circulation.

Patient 2, a 47-year-old woman, was originally diagnosed with bilateral MMD with transient aphasia and right-sided numbness. She underwent left extracranial–intracranial bypass surgery in 2009, which resolved her symptoms. However, follow-up computed tomography (CT) perfusion imaging in 2013 demonstrated right hemisphere hypoperfusion. She participated in our research in 2013 (referred to as her 'pre-operative' scan). She then underwent a right-side encephalo-duro-arterio-synangiosis procedure in 2014, and participated in our research study again 9 months later (referred to as her 'postoperative' scan).

Four women (mean age: 54 ± 5·4) who self-reported as neurologically healthy, served as controls. Written informed consent was obtained from all participants as approved by the McGill Institutional Review Board.

Data acquisition

MRI data were acquired on a 3 T Siemens TIM Trio (32-channel head coil, Erlangen, Germany). A sagittal T1-weighted anatomic image was acquired using MPRAGE. FMRI data were acquired using a dual-echo EPI pseudo-continuous arterial spin labelling (ASL) sequence ($TR/TE_1/TE_2$ = 4000/10/30 ms, label duration/postlabel delay = 1665/900 ms, 3·9 mm isotropic voxels, GRAPPA = 2). CVR was evaluated using RespirAct™ (Slessarev *et al.*, 2007) (Thornhill Research, Toronto, ON, Canada) to target end-tidal CO_2 to 10 mmHg above the participant's baseline while maintaining iso-oxia (56 s baseline, 56 s hypercapnia, 120 s baseline, 120 s hypercapnia and 56 s baseline).

The tasks consisted of viewing a reversing radial checkerboard (8 Hz), bilateral sequential finger tapping (2 Hz, cued by metronome) or both simultaneously (all tasks consisted of 16 s baseline, followed by four repetitions of 40 s on/40 s baseline). In all tasks, participants were instructed to maintain gaze on a central fixation point. Finger tapping on/off blocks were visually cued by the checkerboard in the combined task, and by the colour of the fixation point in the separate motor task. Visual stimuli were presented using PsychoPy (Peirce, 2008). Tapping performance was monitored via video to ensure that all participants approximately maintained the correct tapping frequency at all times.

Data analysis

Spatial preprocessing (motion correction and spatial smoothing, 5 mm FWHM) was performed using the ASLtbx (Wang *et al.*, 2008) in SPM8. Registration to the T1-weighted image and standard space and generation of activation and CVR maps ($z > 2·3$, $P<0·05$, corrected) were performed in FSL's FEAT (Jenkinson & Smith, 2001; Woolrich *et al.*, 2001; Worsley, 2001; Jenkinson

et al., 2002; Smith, 2002; Smith *et al.*, 2004; Andersson *et al.*, 2007). A boxcar function of the task/CO_2 was convolved with a gamma function (task: standard deviation = 3 s, mean lag = 6 s; CO_2: standard deviation = 15, mean lag = 30 s) to model the responses. A linear term was included as a nuisance regressor in the model to account for signal drift.

Four regions of interest (ROIs) were defined using an atlas (Desikan *et al.*, 2006): left and right primary sensorimotor cortices (motor ROIs) and intracalcarine sulci (visual ROIs). For each task, laterality indices (LI) in the motor and visual ROIs were calculated based on activation extent (LI = +1: left activation only; LI = 0: symmetric activation; LI = −1: right activation only) (Cramer *et al.*, 1997). All tasks were expected to activate an approximately symmetric bilateral network with regard to neural activity.

Results

All participants were able to maintain the tapping frequency in both the separate motor task and the combined task.

With respect to the ASL data, apparent hyperperfusion in affected regions in patient 1 (data not shown) suggested intravascular artefacts due to increased transit time, a known ASL artefact in MMD (Wang *et al.*, 2014). Statistically significant perfusion-weighted signal was not detected in MMD-affected regions for patient 2. All subsequent analyses are performed on the BOLD data only.

Laterality indices for controls and presurgery patient data are summarized in Fig. 1. As expected, bilateral activation of visual and motor ROIs was observed for all controls, for all tasks (mean LI: 0·04 ± 0·12; Fig. 1). An example control subject's CVR and task-related activation for sensorimotor and visual regions can be found in Figs 2a and 3a, respectively. Presurgery, patients with MMD had abnormal CVR localized in right anterior/middle territories as expected (Fig. 2b,c, top row). Preoperatively, patient 1's motor ROI activation was slightly left-lateralized for the motor task (LI = 0·34), and lateralized to an even greater extent in the visual–motor task (LI = 0·81; Fig. 2b). Left-lateralized activation was also observed in the visual ROI for the visual–motor task (visual task LI = 0·17, visual–motor task LI = 0·45), consistent with posterior CVR deficits observed in this patient (Fig. 3b). However, in this case, the increased lateralization in the visual–motor task was driven mainly by increased activation extent in the unaffected left hemisphere in the visual–motor task (left visual ROI: 11 688 mm^3; right visual ROI 4416 mm^3) compared to the visual task (left visual ROI: 5184 mm^3; right visual ROI: 3656 mm^3).

For patient 2, activation of the motor ROIs during the motor task was approximately bilaterally symmetric (LI = −0·02); however, activation in the right motor ROI (i.e. affected region) was greatly reduced in the visual–motor task compared to the motor task (LI = 0·99; Fig. 2c). Visual ROI activation for patient 2 was relatively symmetric for both the visual (LI = 0·14) and visual–motor tasks (LI = 0·08), consistent with normal appearing CVR in this region (Fig. 3c).

Postoperative images for both patients can be found in Fig. 4. Postoperatively, patient 1's motor ROI activation was more bilateral for both the motor (LI = 0·20) and visual–motor (LI = 0·34) tasks, consistent with improvement of CVR in the right motor cortex (Fig. 4b).

Postoperatively, patient 2's CVR in primary sensorimotor regions was reduced relative to the preoperative scan. The extent of voxels with positive CVR response decreased from 74 360 mm^3 preoperatively to 34 152 mm^3 postoperatively in the left motor ROI, and 31 008 mm^3 preoperatively to 24 056 mm^3 postoperatively in the right motor ROI. However, we did observed increased CVR postoperatively in a small region over the right anterior frontal lobe (Fig. 4d top row); this area was also associated with a small cluster of right motor ROI activation during the motor task (Fig. 4d, middle row, pink circle). In general, activation extent was greatly reduced in the

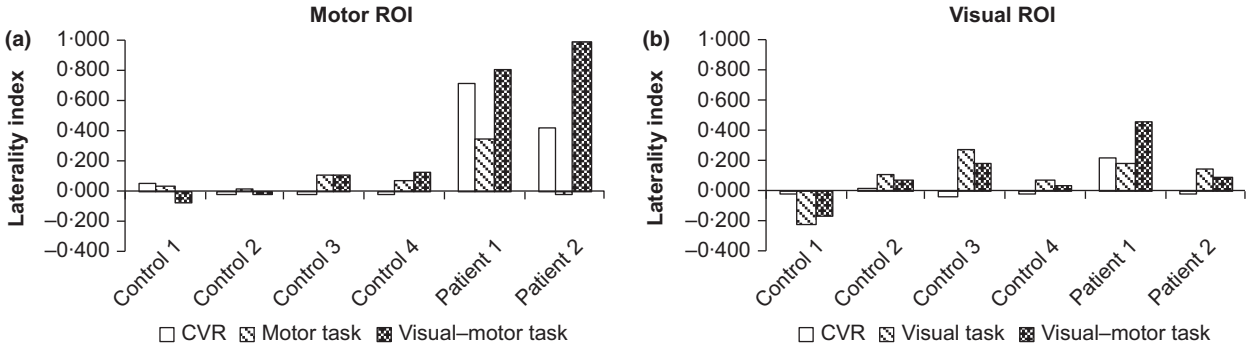

Figure 1 Laterality indices (1 = completely left-lateralized activation; 0 = bilateral activation; −1 = completely right lateralized activation) for the four controls and two patients (preoperative data only), calculated based on the activation extent (i.e. number of significantly activated voxels). Only positive responses are considered here. a: Motor ROI; b: Visual ROI. The controls had approximately bilateral activation in both ROIs for both the separate and combined tasks, consistent with bilaterally distributed CVR. In patient 1, the motor ROI CVR was left-lateralized. In addition, activation was left-lateralized in both tasks, but to a greater extent in the combined task. This pattern was also observed to a lesser extent in the visual ROI in this patient. In patient 2, the motor ROI had left-lateralized CVR, bilateral activation in the separate motor task and left-lateralized activation in the combined visual–motor task. CVR in the visual ROI was normal in this patient, consistent with approximately bilateral activation in both the separate visual and combined visual–motor task).

motor ROIs postoperatively. In the motor task, activation extent decreased from 12 728 mm^3 preoperatively to 0 mm^3 postoperatively in the left motor ROI and 13 232 mm^3 preoperatively to 3920 mm^3 postoperatively in the right motor ROI. No postoperative activation was observed in the motor ROI during the visual–motor task (Fig. 4d bottom row).

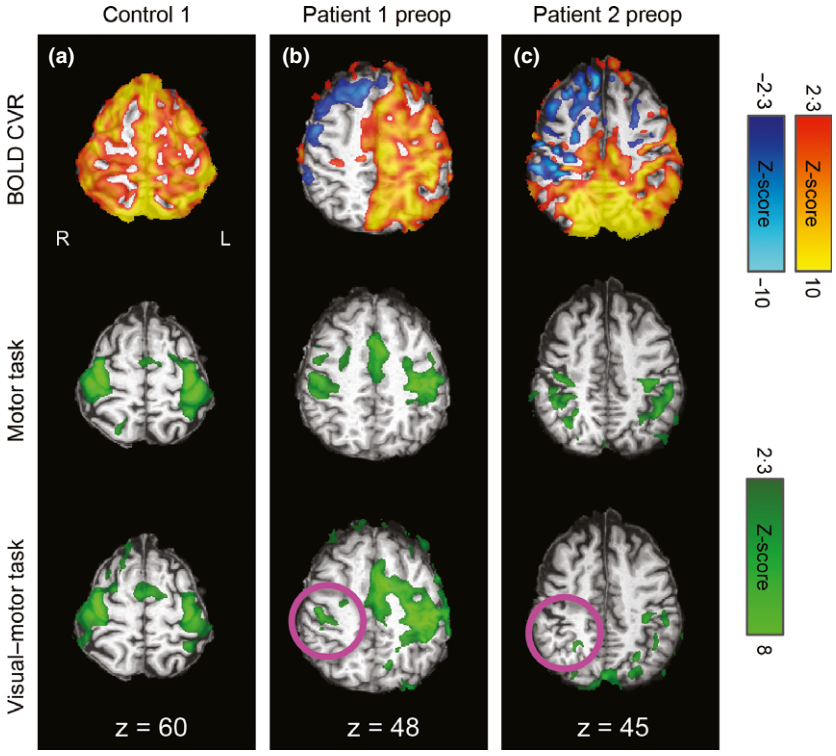

Figure 2 CVR and task-related activation maps overlaid on the individuals' T1-weighted images in standard space for sensorimotor regions. R=right, L=left, coordinates refer to MNI space. Motor cortex CVR (top row) and task-related activation during the separate motor task (middle row) and combined visual–motor task (bottom row) for an illustrative control (a), patient 1 preoperatively (b), and patient 2 preoperatively (c). Robust positive CVR was observed in the control, whereas the patients had large areas of negative or absent CVR, particularly over the affected (right) hemispheres. As expected, task activation was bilateral in the control participant (a). In the patients (b and c), activation was more lateralized during the combined task than the separate task, with reduced or absent activation over the affected hemisphere during the combined task (pink circles).

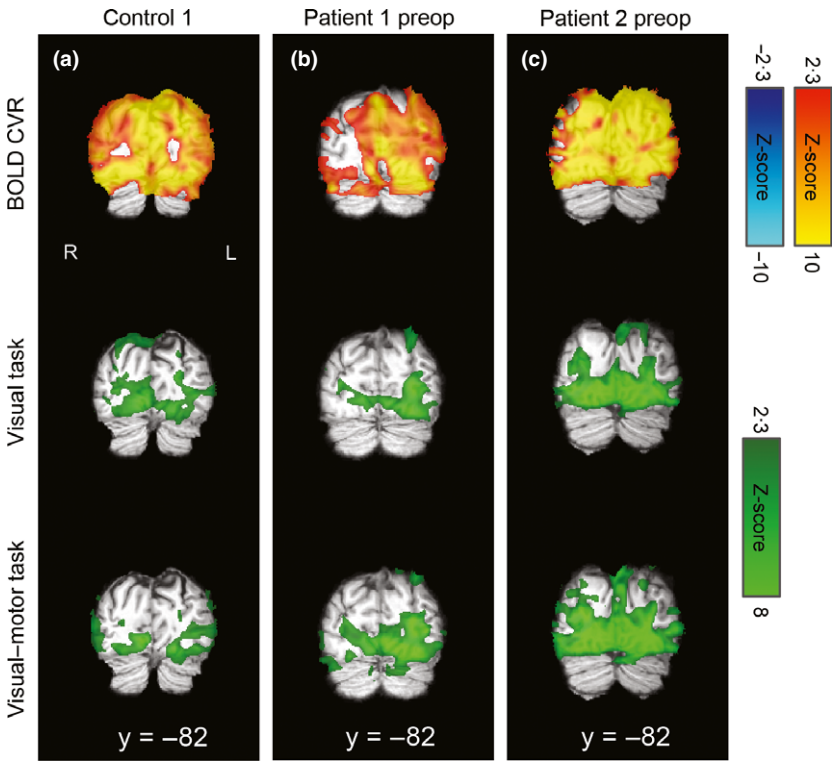

Figure 3 CVR and task-related activation maps overlaid on the individuals' T1-weighted images in standard space for visual regions. R=right, L=left, coordinates refer to MNI space. Visual cortex CVR was robustly positive in the illustrative control (a) and patient 1 (b), who both demonstrated bilateral visual activation for both the separate visual task and combined visual–motor task. There were some posterior areas with reduced/absent CVR in patient 2 (c), which corresponded to more lateralized responses, particularly in the visual–motor task, for this patient and ROI (see text and Fig. 1 for details).

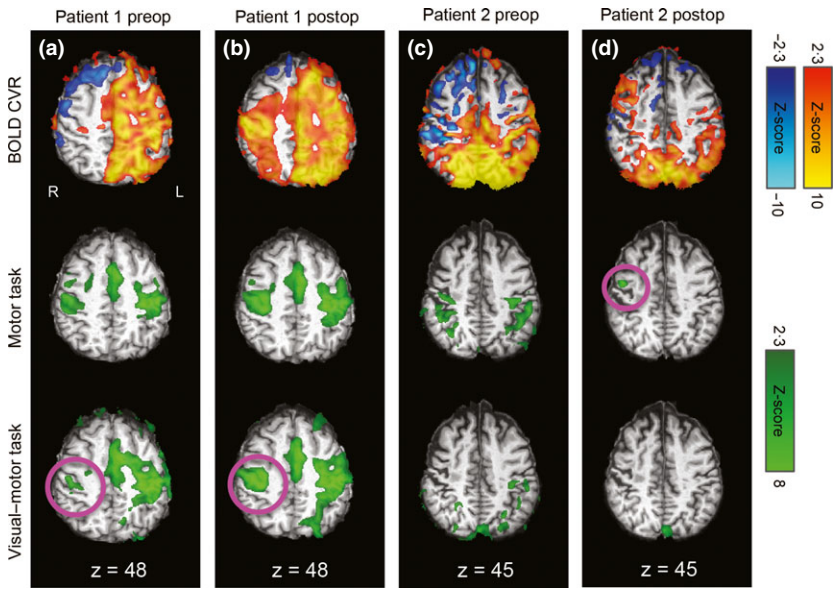

Figure 4 Postoperative results from sensorimotor regions for patients 1 and 2 (panels b and d), with preoperative data repeated here for ease of comparison (panels a and c). R=right, L=left, coordinates refer to MNI space. Postoperatively, patient 1's activation pattern was more bilateral in both tasks, but this was particularly true for the combined task. This was consistent with improved CVR over the affected hemisphere (panel B). Patient 2's CVR was reduced postoperatively, except in a right anterior region, which was also associated with activation in the motor task (panel D, pink circle).

Discussion

Preliminary data from two patients with MMD and four controls showed that task-related fMRI activation in regions with abnormal CVR was dependent on the total vascular demands of the task. Task-related BOLD responses in MMD-affected regions were reduced or absent during a combined visual–motor task associated with both local and remote vascular demands, but relatively normal in a separate motor task associated with local vascular demands only. In patient 1, we observed that both CVR and task-related fMRI activation were restored after bypass surgery. In patient 2, CVR was reduced in sensorimotor regions after revascularization surgery, and task-related activation in these regions was also greatly reduced. These observations associated with revascularization surgery provide additional evidence of the hemodynamic origin of this effect. Future work in which perfusion changes are measured directly with ASL would be of great value for understanding the relationships among pathology, neurovascular coupling and CVR. However, assessing perfusion with ASL is very challenging in areas of hypoperfusion and/or increased transit time. Overcoming these limitations will be crucial to future applications of ASL in cerebrovascular disease.

Given that patients performed the motor task equally well in both the separate and combined conditions (as assessed via videos of finger tapping demonstrating that tapping rate remained approximately the same across tasks), the decreased fMRI activation in the affected primary sensorimotor cortex during the combined task is unlikely to reflect differences in neural activity. While it is possible that greater laterality during the combined task could have arisen from factors other than variations in neurovascular coupling, it is difficult to identify a plausible alternative within the context of our design. Neural plasticity and/or functional reorganization are unlikely to have occurred on the time scale of our experiment. Likewise, factors such as learning and habituation are unlikely to manifest as laterality differences in bilateral finger tapping tasks.

Our findings demonstrate the impact of variations in neurovascular coupling on comparisons of cerebrovascular disease patients and controls, as well as longitudinal studies of such patients. Incorporating CVR measurements may be useful for future fMRI studies of patients with cerebrovascular disease to identify regions of potential neurovascular uncoupling. Furthermore, by studying patients with MMD, in whom affected and unaffected regions follow a characteristic spatial distribution, we were able to demonstrate the effects of remote vascular demands on BOLD fMRI activation results using simple sensorimotor and visual tasks. In this way, MMD can be thought of as a 'model system' for studying the effects of remote vascular demands; however, we expect that analogous effects occur in other diseases. In cases with affected regions localized to association areas, or more globally distributed disease, it may be more challenging to design tasks to probe the impact of remote vascular demands.

Our findings also have implications for interpreting CVR results. Negative BOLD CVR is generally thought to reflect vascular steal. While this has been suggested to indicate that the vessels are in a chronic state of maximal dilation and cannot react to a vasodilator (Poublanc *et al.*, 2013), our results demonstrate that regions of negative CVR can still exhibit BOLD signal increases in response to task-related demands under certain conditions, suggesting the persistence of some vasodilatory control. This finding tempers previous speculations that regions of negative CVR suffer from chronic neurovascular uncoupling (Mikulis, 2013) and highlights the complexities of evaluating cerebrovascular health. Within a typical CVR experiment, regional CVR values depend on both the local vasculature's capacity to respond, as well as flow redistribution among other vascular territories. Regional CVR values therefore do not solely reflect the local vasculature's ability to respond to neural activity, but

rather the net local response to a global stimulus. Parametric tests of brain function, such as task batteries or graded vasodilatory challenges, may be useful for understanding the full range of vascular responses in patients.

Acknowledgments

The authors gratefully acknowledge the contributions of D. Costa, M. Ferreira, R. Lopez and L. Marcotte for assistance with data collection. Thanks are extended to J. J. Wang for providing the dual-echo pseudo-continuous ASL sequence and M.E. McCowan for editorial support. We acknowledge research funding support from the Canadian Imperial Bank of Commerce Fellowship in Brain Imaging, Alberta Innovates-Health Solutions, The Natural Sciences and Engineering Council of Canada, The Canadian Institutes of Health Research and The Campus Alberta Innovates Program.

Conflict of interests

The authors have no conflict of interests.

References

Andersson JL, Jenkinson M, Smith S, *et al.* Non-linear registration, aka Spatial normalisation FMRIB technical report TR07JA2. FMRIB Anal Group Univ Oxf (2007); Available at: http://fmrib.medsci.ox.ac.uk/analysis/techrep/tr07ja2/tr07ja2.pdf [Accessed August 5, 2015].

Arteaga DF, Strother MK, Faraco CC, *et al.* The vascular steal phenomenon is an incomplete contributor to negative cerebrovascular reactivity in patients with symptomatic intracranial stenosis. *J Cereb Blood Flow Metab* (2014); **34**: 1453–1462.

Blair GW, Doubal FN, Thrippleton MJ, *et al.* Magnetic resonance imaging for assessment of cerebrovascular reactivity in cerebral small vessel disease: a systematic review. *J Cereb Blood Flow Metab* (2016); **36**: 833–841.

Burke GM, Burke AM, Sherma AK, *et al.* Moyamoya disease: a summary. *Neurosurg Focus* (2009); **26**: E11.

Calautti C, Baron J-C. Functional neuroimaging studies of motor recovery after stroke in adults: a review. *Stroke* (2003); **34**: 1553–1566.

Chen JJ, Pike GB. Global cerebral oxidative metabolism during hypercapnia and hypocapnia in humans: implications for BOLD fMRI. *J Cereb Blood Flow Metab* (2010); **30**: 1094–1099.

Cramer SC, Nelles G, Benson RR, *et al.* A functional MRI study of subjects recovered from hemiparetic. *Stroke* (1997); **28**: 2518–2527.

Desikan RS, Ségonne F, Fischl B, *et al.* An automated labeling system for subdividing the human cerebral cortex on MRI scans into gyral based regions of interest. *NeuroImage* (2006); **31**: 968–980.

Geranmayeh F, Wise RJS, Leech R, *et al.* Measuring vascular reactivity with breath-holds after stroke: a method to aid interpretation of group-level BOLD signal changes in longitudinal fMRI studies. *Hum Brain Mapp* (2015); **36**: 1755–1771.

Hodics T, Cohen LG, Cramer SC. Functional imaging of intervention effects in stroke motor rehabilitation. *Arch Phys Med Rehabil* (2006); **87**: 36–42.

Jenkinson M, Smith S. A global optimisation method for robust affine registration of brain images. *Med Image Anal* (2001); **5**: 143–156.

Jenkinson M, Bannister P, Brady M, *et al.* Improved optimization for the robust and accurate linear registration and motion correction of brain images. *NeuroImage* (2002); **17**: 825–841.

Miki A, Nakajima T, Takagi M, *et al.* Functional magnetic resonance imaging of visual cortex in a patient with cerebrovascular insufficiency. *Neuro-Ophthalmol* (2000); **23**: 83–88.

Mikulis DJ. Chronic neurovascular uncoupling syndrome. *Stroke* (2013); **44**: S55–S57.

Peirce JW. Generating stimuli for neuroscience using PsychoPy. *Front Neuroinform* (2008); **2**: 10.

Pike GB. Quantitative functional MRI: concepts, issues and future challenges. *NeuroImage* (2012); **62**: 1234–1240.

Poublanc J, Han JS, Mandell DM, *et al.* Vascular steal explains early paradoxical blood oxygen level-dependent cerebrovascular response in brain regions with delayed arterial transit times. *Cerebrovasc Dis Extra* (2013); **3**: 55–64.

Richards LG, Stewart KC, Woodbury ML, *et al.* Movement-dependent stroke recovery: a systematic review and meta-analysis of TMS and fMRI evidence. *Neuropsychologia* (2008); **46**: 3–11.

Sam K, Small E, Poublanc J, *et al.* Reduced contralateral cerebrovascular reserve in patients with unilateral steno-occlusive disease. *Cerebrovasc Dis* (2014); **38**: 94–100.

Scott RM, Smith ER. Moyamoya disease and moyamoya syndrome. *N Engl J Med* (2009); **360**: 1226–1237.

Slessarev M, Han J, Mardimae A, *et al.* Prospective targeting and control of end-tidal CO2 and O2 concentrations. *J Physiol* (2007); **581**: 1207–1219.

Smith SM. Fast robust automated brain extraction. *Hum Brain Mapp* (2002); **17**: 143–155.

Smith SM, Jenkinson M, Woolrich MW, *et al.* Advances in functional and structural MR image analysis and implementation as FSL. *NeuroImage* (2004); **23**(Suppl 1): S208–S219.

Sobczyk O, Battisti-Charbonney A, Fierstra J, *et al.* A conceptual model for CO_2-induced redistribution of cerebral blood flow with experimental confirmation using BOLD MRI. *NeuroImage* (2014); **92**: 56–68.

Spano VR, Mandell DM, Poublanc J, *et al.* CO2 blood oxygen level-dependent MR mapping of cerebrovascular reserve in a clinical population: safety, tolerability, and technical feasibility. *Radiology* (2013); **266**: 592–598.

Stinear C. Prediction of recovery of motor function after stroke. *Lancet Neurol* (2010); **9**: 1228–1232.

Uchino K, Johnston SC, Becker KJ, *et al.* Moyamoya disease in Washington State and California. *Neurology* (2005); **65**: 956–958.

Veldsman M, Cumming T, Brodtmann A. Beyond BOLD: optimizing functional imaging in stroke populations. *Hum Brain Mapp* (2015); **36**: 1620–1636.

Wang Z, Aguirre GK, Rao H, *et al.* Empirical optimization of ASL data analysis using an ASL data processing toolbox: ASLtbx. *Magn Reson Imaging* (2008); **26**: 261–269.

Wang R, Yu S, Alger JR, *et al.* Multi-delay arterial spin labeling perfusion MRI in moyamoya disease–comparison with CT perfusion imaging. *Eur Radiol* (2014); **24**: 1135–1144.

Woolrich MW, Ripley BD, Brady M, *et al.* Temporal autocorrelation in univariate linear modeling of FMRI data. *NeuroImage* (2001); **14**: 1370–1386.

Worsley KJ. Statistical analysis of activation images. In *Functional MRI: An Introduction to Methods* (eds Jezzard, P, Matthews, PM) (2001), pp. 251–270. Oxford University Press, New York.

Zappe AC, Uludağ K, Logothetis NK. Direct measurement of oxygen extraction with fMRI using 6% CO2 inhalation. *Magn Reson Imaging* (2008); **26**: 961–967.

